Deciphering the proteome of the in vivo diagnostic reagent "purified protein derivative" from Mycobacterium tuberculosis

ARTICLE *in* PROTEOMICS · APRIL 2012

Impact Factor: 3.81 · DOI: 10.1002/pmic.201100544 · Source: PubMed

RESEARCH ARTICLE

Deciphering the proteome of the in vivo diagnostic reagent "purified protein derivative" from *Mycobacterium tuberculosis*

Yun Sang Cho[1,**], Karen M. Dobos[1*], Jessica Prenni[2], Hongliang Yang[1], Ann Hess[3], Ida Rosenkrands[4], Peter Andersen[4], Sung Weon Ryoo[5], Gill-Han Bai[5], Michael J. Brennan[6**], Angelo Izzo[1], Helle Bielefeldt-Ohmann[1**] and John T. Belisle[1]*

[1] Mycobacteria Research Laboratories, Department of Microbiology, Immunology, and Pathology, Colorado State University, Fort Collins, CO, USA
[2] Proteomics and Metabolomics Facility, Colorado State University, Fort Collins, CO, USA
[3] Department of Statistics, Colorado State University, Fort Collins, CO, USA
[4] Department of Infectious Disease Immunology, Statens Serum Institut, Copenhagen S, Denmark
[5] Korea Institute of Tuberculosis, Seoul, Republic of Korea
[6] Laboratory of Mycobacterial Diseases and Cellular Immunology, Center for Biologics Evaluation and Research, Food and Drug Administration, Bethesda, MD, USA

Received: October 13, 2011
Revised: December 30, 2011
Accepted: January 10, 2012

Purified protein derivative (PPD) has served as a safe and effective diagnostic reagent for 60 years and is the only broadly available material to diagnose latent tuberculosis infections. This reagent is also used as a standard control for a number of in vitro immunological assays. Nevertheless, the molecular composition and specific products that contribute to the extraordinary immunological reactivity of PPD are poorly defined. Here, a proteomic approach was applied to elucidate the gene products in the U.S. Food and Drug Administration (FDA) standard PPD-S2. Many known *Mycobacterium tuberculosis* T-cell antigens were detected. Of significance, four heat shock proteins (HSPs) (GroES, GroEL2, HspX, and DnaK) dominated the composition of PPD. The chaperone activities and capacity of these proteins to influence immunological responses may explain the exquisite solubility and immunological potency of PPD. Spectral counting analysis of three separate PPD reagents revealed significant quantitative variances. Gross delayed-type hypersensitivity (DTH) responses in *M. tuberculosis* infected guinea pigs were comparable among these PPD preparations; however, detailed histopathology of the DTH lesions exposed unique differences, which may be explained by the variability observed in the presence and abundance of early secretory system (Esx) proteins. Variability in PPD reagents may explain differences in DTH responses reported among populations.

Keywords:
DTH / Microbiology / *Mycobacterium tuberculosis* / PPD

Correspondence: Dr. John T. Belisle, Mycobacteria Research Laboratories, Department of Microbiology, Immunology, and Pathology, Colorado State University, Fort Collins, CO 80523-1690, USA
E-mail: jbelisle@colostate.edu
Fax: +1-970-491-8707

Abbreviations: DTH, delayed-type hypersensitivity; **HSPs**, heat shock proteins; **KIT**, Korea Institute of Tuberculosis; **PPD**, purified protein derivative; **RA**, reduced and alkylated; **RAC**, reduced, alkylated, and chymotrypsin digested; **RAT**, reduced, alkylated, and trypsin digested; **RP**, reversed phase; **SCX**, strong cation exchange; **SSI**, Statens Serum Institute; **TU**, tuberculin units; **UN**, untreated

*These authors contributed equally to this work.
**Current addresses: Dr. Yun Sang Cho, Foreign Animal Disease Division, Animal, Plant and Fisheries Quarantine and Inspection Agency, Anyang 430-757, Republic of Korea.
Dr. Michael J. Brennan, AERAS Global Tuberculosis Foundation, Rockville, MD 20850, USA.
Dr. Helle Bielefeldt-Ohmann, School of Veterinary Science, University of Queensland, Gatton Campus; Gatton, Qld 4343, Australia.

1 Introduction

Tuberculosis is a disease in humans and other vertebrates that progresses through complex interactions between the host's immune system and the pathogenic bacterium *Mycobacterium tuberculosis*. In particular, the induction of a prominent inflammatory response as well as a strong adaptive immune response by *M. tuberculosis,* are hallmarks of this disease. Early after the discovery of *M. tuberculosis* as the causative agent of tuberculosis, Robert Koch introduced tuberculin as a potential vaccine against tuberculosis [1]. This material was a crude mixture of macromolecules produced by *M. tuberculosis* and released into the culture medium upon heat inactivation of the bacterium. Tuberculin failed as a vaccine because it elicited a damaging immune response known as the "Koch phenomenon" in individuals already infected with *M. tuberculosis*. However, this same immune-mediated event was later recognized as having diagnostic value [2] based on observations that tuberculin produced localized edema within 1–2 days of its injection into the skin of animals infected with *M. tuberculosis*. This classical immunological reaction now known as delayed-type hypersensitivity (DTH) or Type IV hypersensitivity has served for nearly a century as the primary basis for diagnosing (via the cellular immune response) exposure to *M. tuberculosis*.

The seminal work of Florence Seibert revealed that the tuberculosis-specific DTH response induced by tuberculin was attributable to the "tuberculoprotein" [3]. Her work also led to refined production techniques that minimized carbohydrate and nucleic acid contamination and inconsistencies in the reactivity of tuberculin preparations [4]. The material produced in 1941 by Seibert established modern day purified protein derivative (PPD) and the first international standard, PPD-S1. From this, additional standards were produced to include RT23 by the Statens Serum Institut (SSI) [5, 6] and the replenishment of the PPD-S1 with PPD-S2 [7]. While each lot of PPD meets specific standards for biological activity [7], early studies noted significant differences in potency among standard PPD preparations [5]. Chemical analyses of standard PPD preparations also demonstrate significant compositional differences. Specifically, PPD-S2 is comprised of 93% protein, 1% nucleic acid, and 6% carbohydrate. In comparison, PPD RT-23 from the SSI was 80% protein, 20% nucleic acid, and <1% carbohydrate (M.J. Brennan, unpubl. data).

Identification of a selected number of individual proteins or protein fragments present in PPD has been reported [8–11]. However, a comprehensive identification of all proteins represented in human PPD does not exist. This is in sharp contrast to the evaluation of *M. tuberculosis*, where extensive proteomic studies have been performed to characterize the protein profile of this bacterium with respect to subcellular location [12–15], differences among strains [16–21], alterations associated with growth conditions [22–29], and elucidation of antigens for the cellular and humoral immune responses [30–34]. A complete understanding of the molecular composition of PPD would not only allow for the construction of a more refined skin test antigen, but it may also provide insight as to why PPD elicits such a vigorous immune response. A major impediment to the molecular definition of PPD is the fact that this material is a mixture of denatured, but soluble proteins and peptides that are generated through autoclaving in vitro grown *M. tuberculosis* at 100°C for 2 h. Thus, individual proteins of PPD cannot be resolved by SDS-PAGE or 2D-PAGE. Kuwabara reported the purification of a dominant 9.7 kDa protein of PPD that exhibited strong DTH activity and further provided the sequence of this protein by N-terminal sequencing of selected peptides [10, 11] However, these reported sequences are now known not to represent any mycobacterial protein [35] nor to be encoded by the *M. tuberculosis* genome [36]. This example underscores the complexity of PPD and the technical difficulties that have been associated with defining its composition.

Modern multidimensional chromatography techniques [37] coupled to soft ionization mass spectrometry (MS) technologies [38] and powerful computer algorithms to search tandem mass spectrometry (MS/MS) data against protein databases [39, 40] have allowed for the facile identification of proteins within complex mixtures such as tissue lysates or subcellular fractions. Quantitative approaches such as spectral counting [41] and isotope tagging [42] have also allowed for the relative quantities of individual proteins to be determined within and between complex protein preparations. We have now applied these approaches to decipher the protein composition of the standard PPD preparation, PPD-S2, and found that it possessed at least 240 protein representatives, with four proteins (GroES, GroEL2, HspX, and DnaK) dominating this composition. Our studies also reveal that spectral counting analysis is capable of distinguishing significant variability in the composition of standard PPD preparations, and that these variations may impact the biological activity.

2 Materials and methods

2.1 Reduction, alkylation, and trypsin and chymotrypsin digestion of PPD

Standard PPD-S2 was provided from the U.S. FDA, PPD-RT23, was provided by the SSI, and PPD-KIT, was provided by the Korea Institute of Tuberculosis (KIT). For comprehensive analysis of PPD, PPD-S2 was reduced with DTT (Sigma-Aldrich, St. Louis, MO), and alkylated with iodoacetamide (Sigma-Aldrich) by standard methods [43]. Briefly, aliquots (1 mg) of lyophilized PPD-S2 were dissolved in 1 mL of 6 M guanidium hydrochloride (Pierce Chemical Co, Rockford, IL, USA), 0.6 M Tris-HCl, pH 8.6, to which 1 μL of 4 M DTT was added and incubated for 3 h at 23°C. Reduced PPD was alkylated by addition of 100 μL iodoacetamide (160 mM) in HPLC grade water and incubated in the dark for 30 min at 37°C. The reduced and alkylated (RA) PPD was desalted by microdialysis using 50 mM ammonium bicarbonate (pH 7.8) for 48 h. The samples were dried under a vacuum and suspended in 10% ACN, 0.2 M ammonium bicarbonate. Trypsin

or chymotrypsin were added to individual samples at 1:50 enzyme:substrate ratio, and the samples incubated at 37°C and 23°C for 18 h, respectively. This resulted in reduced, alkylated, and trypsin digested (RAT); and reduced, alkylated, and chymotrypsin digested (RAC) PPD. Similarly, three aliquots (100 μg each) of PPD-RT23, PPD-KIT, and PPD-S2 were reduced, denatured, and digested with trypsin as above for quantitative analysis by spectral counting.

2.2 SDS-PAGE and Western blot

Aliquots (10 μg) of PPD, RA PPD, and RAT- and RAC-PPD were resolved by electrophoresis on 4–12% Bis-Tris polyacrylamide gels (Invitrogen, Carlsbad, CA, USA) using denaturing conditions and MES running buffer per manufacturer's instructions. Proteins were visualized by staining with silver nitrate. For Western blot analyses, aliquots (10 μg) of PPD-S2 and a preparation of *M. tuberculosis* cytosolic protein [44] were resolved by SDS-PAGE as above, electroblotted to nitrocellulose, and probed with *M. tuberculosis*-specific monoclonal antibodies SA-12 (anti-GroES), CS-49 (anti-HspX), IT-56 (anti-GroEL2), and IT-41 (anti-DnaK). Antigen detection was visualized with BCIP after incubating blots with antimouse IgG conjugated to alkaline phosphatase.

2.3 In-gel digestion

An aliquot (100 μg) of RAC-PPD was resolved by SDS-PAGE, stained by Coomassie blue R-250, and destained by 50% methanol. Three protein bands, 15, 25, and 37 kDa, were excised and digested in gel with trypsin. The resulting peptides were extracted per standard methods [45].

2.4 2D-LC

RAT- and RAC-PPD were fractionated by strong cation exchange (SCX) chromatography using a polysulfoethyl A™ column (The Nest Group, Southborough, MA, USA) and a Waters Alliance HPLC system. Peptides were eluted by stepwise fractionation at 0, 0.025, 0.05, 0.1, 0.2, and 0.5 M KCl at a flow rate of 1 mL/min. SCX fractions (six per sample) were dried under vacuum to 100 μL and further separated by reversed phase (RP)-HPLC using a Vydac C18 column (The Nest Group) and a linear gradient of ACN (0–80%) in 0.1% TFA. Fractions were collected manually based on peak intensity monitored at A_{214}. The number of individual fractions collected varied per run, and ranged from 16 to 40 per injection.

2.5 Protein identification in PPD-S2 by MS

Comprehensive analysis of PPD-S2 to identify its molecular content was performed by taking an aliquot of each 2D-LC fraction and applying it to a C18 capillary RP-HPLC column in-line with a ThermoFinnigan LCQ electrospray ionization (ESI) mass spectrometer (Thermo Electron, Waltham, MA, USA) as described previously [30]. Briefly, an aliquot (10 μl) of the peptide mixture was injected onto a capillary (0.2–50 mm) C_{18} RP column (Microchom BioResources, Auburn, CA, USA) and eluted with an increasing gradient (5–70%) of acetonitrile in 0.1% acetic acid using an Eldex MicroPro capillary HPLC system (Napa, CA, USA) with a flow rate of 5 μL/min. The RP eluent was introduced directly into ThermoFinnigan LCQ ESI mass spectrometer operated using Xcalibur software version 1.3, and the peptides were analyzed by MS/MS. The electrospray needle was set at 4 kV with a N_2 sheath gas flow of 40 and a capillary temperature of 200°C. MS/MS was automatically performed on the most dominant ion of the previous scan, and the normalized collision energy was set at 40%.

2.6 Database searching

MS/MS data were extracted, deconvoluted, and deisotoped by BioWorks version 3.3. The resulting .dta files were searched against the *M. tuberculosis* protein database (R6, 3993 entries; Genbank accession #AL123456) using SEQUEST (ThermoFinnigan, San Jose, CA, USA; version 27, rev. 12), and MASCOT (Matrix Science, London, UK; version: 2.1 MASCOT) programs. Search parameters included fragment ion mass tolerance of 1.00 Da, parent ion tolerance of 2.5 Da, and variable modifications of oxidation of methionine, and iodoacetamide or iodoacetic derivatives of cysteine for all samples, and acrylamide modification of cysteine for in-gel digested protein bands.

Scaffold (version Scaffold-3_00_01, Proteome Software Inc., Portland, OR, USA) was used to validate MS/MS-based peptide and protein identifications. Peptide identifications were accepted if they achieved the MASCOT program thresholds of 20, 30, and 40 or greater ion score for +1, +2, and +3 charged peptides, respectively, or achieved the Sequest program thresholds of a dCN of 0.1 or greater and 1.5, 2.5, and 3.0 or greater for +1, +2, and +3 charged peptides, respectively. Proteins represented by one peptide were validated by manual interrogation of the MS/MS data. Criteria for validation included: (i) there must be a minimum of 80% coverage of theoretical y or b ions (at least five in consecutive order); (ii) there must be an absence of prominent unassigned peaks greater than 5% of the maximum intensity; and (iii) indicative residue-specific fragmentation, such as intense ions N-terminal to proline and immediately C-terminal to aspartate and glutamate, were used as additional parameters of confirmation. Proteins that contained similar peptides and could not be differentiated based on MS/MS analysis alone were grouped to satisfy the principles of parsimony.

The false discovery rate (FDR) was determined for the comprehensive PPD-S2 dataset by searching the 357

individual .raw files against a decoy database that contained a reversed version of the proteins included in the customized database composed from the *M. tuberculosis* H37Rv FASTA file (7982 entries). The resulting files were pooled in Scaffold and the analysis was identical to that described above. A total of nine proteins and 12 spectra matched to the reverse database, resulting in a protein FDR of 3.9% and peptide FDR of 0.3%. The final dataset was defined by 240 unique proteins represented by 3873 spectra in PPD-S2. All MASCOT generic files (MGF) containing MS/MS spectra are available on PRoteomics IDEntifications database [46] (PRIDE; http://www.ebi.ac.uk/pride/, Accession numbers 19499 and 19500) for review. The scaffold file, containing all compiled, compressed PPD-S2 data, is available at http://www.mrl.colostate.edu/mtb_db/pages/ppd.aspx.

For determination of the ten most dominant protein representatives in PPD-RAC and PPD-RAT, normalized spectral abundance factors were determined [47]. Quantitative values were then assigned for each RAC-PPD and RAT-PPD identified protein so that the two preparations could be directly compared [48].

2.7 Quantitative comparison of separate PPDs by MS

Individual digests of PPD-S2, PPD-RT23, and PPD-KIT were analyzed by LC-MS using a nanospray LC-LTQ as described previously [49]. Each sample was injected in triplicate, resulting in each PPD being represented by nine individual datasets.

Spectrum counting was used to compare PPD-S2, PPD-RT23, and PPD-KIT relative protein abundances. Each sample was represented by a total of nine injections (three biological replicates of each injected three times each). Each injection was interrogated individually using the MASCOT and SEQUEST algorithms as described above. The data were pooled such that each biological replicate included the pooled spectral data from the three injections. The resulting spectra were qualified and validated as described above. All MGF containing MS/MS spectra are available on PRIDE [46] (http://www.ebi.ac.uk/pride/, Accession numbers 19499 and 19500) for review. The scaffold file, containing all compiled, compressed PPD spectral counting data, is available at http://www.mrl.colostate.edu/mtb_db/pages/ppd.aspx.

Total spectral counts from the validated dataset were exported for statistical analysis using Dante (version 1.2, Battelle Memorial Institute). Briefly, individual datasets for each injection were quantile normalized and data compressed for each biological replicate. Replicates were analyzed against each PPD to generate hierarchical clustering analysis (HCA) heat maps. Pair-wise analysis of variance (ANOVA) analysis for each protein was performed to determine statistically significant changes between samples ($p < 0.05$).

2.8 DTH analysis

Hartley guinea pigs (Charles River Laboratories, North Wilmington, MA, USA) weighing ~450 g were infected with approximately 10–30 cfu of *M. tuberculosis* H37Rv (TMCC# 102) via aerosol delivery using a Madison chamber (University of Wisconsin, Madison, WI, USA). At 10 wk postinfection, guinea pigs were anesthetized, shaved, and injected intradermally with 0.1 mL of PPD (PPD-S2, PPD-SSI, or PPD-KIT) containing 1, 5, 10, or 20 tuberculin units (TU; 1 TU is equal to 0.2 μg/mL protein). Reactions were read at 24, 48, and 72 h and expressed in millimeters of diameter of erythema or induration.

2.9 Histopathology

Skin samples were obtained at 72 h postintradermal injection of PPD. These samples were placed on a piece of paper in cassettes, fixed in 10% neutral-buffered formaldehyde for 72 h, and embedded in paraffin and followed by sectioning. Tissue sections (4–5 μm) were stained with hematoxylene and eosin and examined on an Olympus BX41 microscope equipped with a Q-Color3 camera (Olympus, Center Vally, PA, USA) and Stereo Investigator software (MicroBrightField Inc., Williston, VT, USA). The epidermal, dermal, and subcutaneous changes were assigned a severity score based on the following features: (i) epidermis: basal cell hyperplasia and acanthosis, necrosis or apoptosis, intraepidermal microabscesses, subepidermal clefts, transepithelial leukocyte migration, ortho-, and para-hyperkeratosis; (ii) dermis: edema, collagen necrosis, vasculitis, transendothelial leukocyte migration, neutrophil infiltration, monocyte infiltration, mast cell infiltration, and degranulation; and (iii) subcutis: necrosis, edema, neutrophil infiltration, lymphocyte and plasma cell infiltration, monocyte-macrophage infiltration, and vasculitis. Each feature was scored on a scale of 0–4, and the total score for each sample summed up. Photomicrographs are shown without further manipulations.

3 Results

3.1 Protein composition of PPD-S2

Initial assessment of a standard PPD preparation (PPD-S2) used by the U.S. FDA was performed by SDS-PAGE, but as expected this method was unable to resolve discreet protein bands (Fig. 1A), confirming that protein denaturation and degradation occur during the production process [50]. Similarly, PPD was refractory to 2D-PAGE analyses (data not shown). Thus, we hypothesized that the denatured proteins and representative peptides of PPD could be identified by a nongel-based proteomic approach. PPD-S2 was reduced, alkylated with iodoacetamide, and digested with trypsin or chymotrypsin to yield RAT-PPD or RAC-PPD, respectively.

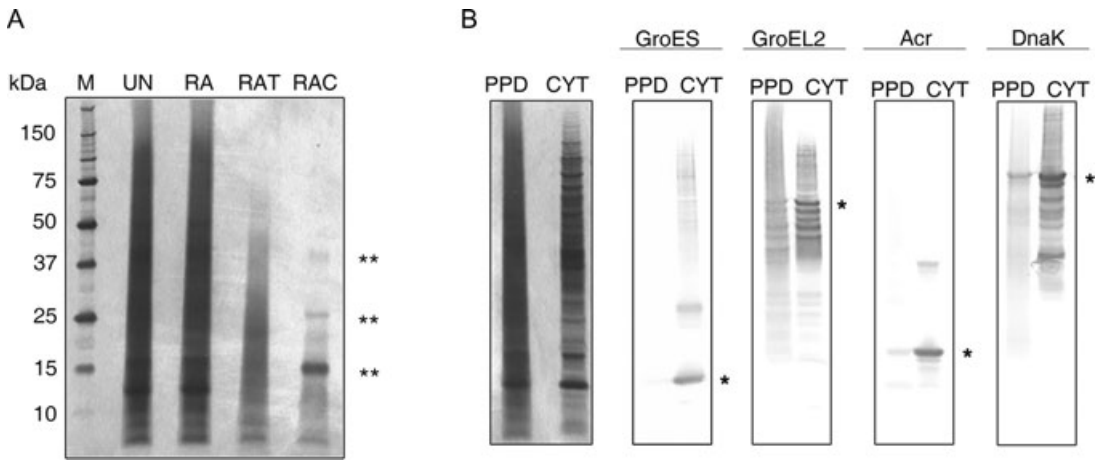

Figure 1. SDS-PAGE and Western blot analyses of PPD-S2 preparations. (A) A silver stained SDS-polyacrylamide gel of PPD-S2 untreated (UN), reduced and alkylated (RA) with iodoacetamide, and digests of the reduced and alkylated material with trypsin (RAT) and chymotrypsin (RAC). The double asterisk marks products that were resistant to chymotrypsin digestion. (B) Western blot analyses of untreated PPD-S2 and the cytosol (CYT) preparation of *M. tuberculosis* for the presence of GroES, GroEL2, Acr (Rv2031c), and DnaK (Rv0350). The left panel is a silver stained gel of PPD-S2 and CYT. The panels marked GroES, GroEL2, Acr, and DnaK are Western blots probed with the monoclonal antibodies SA-12, IT-56, CS-49, and IT-41, respectively.

Analysis of the RAT and RAC-PPD by SDS-PAGE confirmed that both trypsin and chymotrypsin digestion reduced the overall molecular mass of PPD-S2 (Fig. 1A). However, the RAC-PPD displayed three relatively well-resolved bands of ~37, 25, and 15 kDa. In-gel digestion of these products with trypsin and analysis of the resulting peptides by MS/MS revealed that all three bands possessed peptides of GroES (Rv3418c) and the 15 kDa product also contained peptides of GroEL2 (Rv0440) and MPT63 (Rv1926c).

The nongel based proteomic analysis of PPD-S2 was initiated with 2D-LC separation of RAT- and RAC-PPD via SCX- and RP-HPLC. This process yielded 208 and 149 fractions, respectively, for RAT- and RAC-PPD. The 357 2D-LC fractions were resolved by LC coupled to MS/MS and data analyzed by MASCOT and SEQUEST [51]. Statistical validation of peptide assignments using the program thresholds, reduction of spectra by manual interrogation and FDR analysis resulted in identification of 3873 bona fide peptide spectra. Further validation of these using the ProteinProphet algorithm [52] led to identification of 240 protein representatives in PPD-S2 at a confidence level greater than 90%. Thus, we determined that at least 6.0% of coding sequences in the *M. tuberculosis* genome were represented in PPD-S2 (Supporting Information Tables S1 and S2). Of the 240 protein representatives in PPD-S2, 205 and 77 were identified in RAT- and RAC-PPD preparations, respectively, with 75 protein representatives common to both. One hundred seven of the 240 protein representatives identified in PPD were based on a single peptide identified by MS/MS. Stringent criteria (see experimental design) were required for these single peptide hits to be designated as true components of PPD-S2.

3.2 Identification of the most abundant protein representatives of PPD

Our analyses of PPD-S2 demonstrated that a large number (50) of previously identified T-cell antigens were present (Table 1; [53–57]). Given the complexity of PPD it is also expected that T-cell reactivity is largely driven by the most abundant T-cell antigens. Thus, to investigate the relative quantities of individual protein representatives the method of spectral counting [41] was employed. The ten most abundant protein representatives in RAT- and RAC-PPD are shown in Table 2. Of these, nine and eight of the most abundant proteins representatives in RAT- and RAC-PPD, respectively, were known T-cell antigens. Spectral counting also revealed 57.9 and 29.8% of the accepted spectra for RAT- and RAC-PPD, respectively, belonged to four heat shock proteins (HSPs), DnaK (Rv0350), GroEL2 (Rv0440), Acr/HspX (Rv2031c, RAT-PPD only), and GroES (Rv3418c). Analysis of undigested PPD by Western blot confirmed the presence of these four proteins and notably, that they were aggregates and/or partially degraded in PPD (Fig. 1B).

3.3 Biological variability among PPD preparations

Production methods for PPD can vary among manufacturers, and this variability correlates with variance in potency [58]. To examine this phenomenon three PPD preparations (PPD-S2, PPD-RT23, and PPD-KIT produced at the KIT) were assessed for biological activity. Hartley guinea pigs infected with a low dose aerosol of virulent *M. tuberculosis* [59] were injected

Table 1. T-cell antigens of PPD-S2

Rv number	Protein name	Mol. mass (Da)	Ref.
Rv0009	PpiA	19 221.6	[53]
Rv0054	Ssb	17 303.1	[53]
Rv0125	PepA	34 907	[55]
Rv0129c	FbpC2	36 753.8	[54]
Rv0350	DnaK	66 812.9	[54]
Rv0440	GroEL2	56 709.3	[54]
Rv0475	HbhA	21 517.1	[54]
Rv0577	Tb27.3	27 324.5	[53]
Rv0652	RplL	13 422.6	[53]
Rv0667	RpoB	129 200.9	[57]
Rv0685	Tuf	43 542.6	[55]
Rv0733	Adk	20 075.6	[53]
Rv0798c	Cfp29	28 812.9	[54]
Rv0831c	Hypothetical protein	30 171.2	[56]
Rv0934	PhoS1	38 193.8	[54]
Rv0952	SucD	31 211.6	[53]
Rv1211	Hypothetical protein	7792	[53]
Rv1352	Hypothetical protein	12 831.6	[53]
Rv1411c	LprG	24 529.7	[54]
Rv1626	Probable transcriptional regulator	22 651.8	[53]
Rv1827	Cfp17	17 200.5	[54]
Rv1860	ModD	32 702.8	[54]
Rv1886c	FbpB	34 563.6	[54]
Rv1908c	KatG	80 555.9	[54]
Rv1926c	Mpt63	16 495.8	[54]
Rv1932	Tpx	16 878.2	[54]
Rv1980c	Mpt64	24 805.3	[54]
Rv1984c	Cfp21	21 763.9	[54]
Rv2031c	HspX	16 209.6	[54]
Rv2220	GlnA1	53 522	[54]
Rv2346c	EsxO	9935.6	[56]
Rv2376	Cfp2	16 617.0	[56]
Rv2428	AhpC	21 548.7	[53]
Rv2461c	ClpP	21 658.5	[53]
Rv2476c	Gdh	176 884.9	[55]
Rv2626c	Hypothetical protein	15 499.6	[54]
Rv2744c	35kd_ag	29 239.9	[55]
Rv2780	Ald	38 695.2	[55]
Rv2878c	Mpt53	18 364.9	[54]
Rv2945	LppX	24 121.9	[55]
Rv3028c	FixB	31 672	[53]
Rv3029c	FixA	28 062.9	[53]
Rv3418c	GroES	10 754.1	[54]
Rv3763	LpqH	15 096.2	[54]
Rv3804c	FbpA	35 668.3	[54]
Rv3841	BfrB	20 423.6	[53]
Rv3846	SodA	22 984.3	[54]
Rv3874	Cfp10	10 775.6	[54]
Rv3875	Esat6	9885.8	[54]
Rv3914	TrxC	12 526.5	[54]

intradermally with 0.2 μg of each preparation and erythema measured at 24, 48, and 72 h. For all preparations DTH responses were observed at 24 h, increased slightly at 48 h, and began to wane at 72 h (Fig. 2A). A comparison of the mean erythematous responses at each time point did not show significant differences between PPD formulations. However, ANOVA among animals using the Tukey–Kramer post-test analysis demonstrated greater variability in the DTH responses to PPD-KIT and PPD-RT-23 at 48 h compared to PPD-S2, with p-values of 0.034 and 0.026, respectively. Histopathology of skin biopsies from infected animals sampled at 72 h post PPD injection revealed severe inflammatory reactions characterized by edema, fibrin transudation, vasculitis, infiltration of neutrophils, monocyte-macrophages and lymphocytes, and tissue necrosis regardless of the PPD preparation (Fig. 2 B–D). Yet, inflammation was notably more severe in animals receiving PPD-KIT (Fig. 2C) and PPD-RT23 (Fig 2D) as compared to the PPD-S2 (Fig. 2B). The increased inflammation was due to enhanced edema, fibrin transudation, haemorrhage, and very pronounced leukocyte infiltration. Additionally, edema of the subcutis was observed in animals receiving PPD-KIT.

3.4 Compositional variability among PPD preparations

The histological differences in the DTH response may be associated with significant biochemical differences present in PPD preparations. While total carbohydrate, protein, and nucleic acid content are known to vary among PPD preparations (M. J. Brennan, unpubl. data), differences in protein profiles have not been assessed. The complexity and characteristics of the protein representatives in PPD do not allow for classical quantitative proteomic studies, such as 2-D PAGE or Western blot. Nevertheless, the PPD preparations should be amenable to relative quantification via spectral counting [47, 48]. Thus, the three PPD preparations were processed to generate RAT-PPDs and assayed for quantitative differences in their peptide profiles as described in the methods. Three pair-wise PPD combinations (PPD-S2 versus PPD-S2, PPD-RT23 versus PPD-S2, and PPD-KIT versus PPD-S2) were analyzed to identify statistical differences in individual protein abundance between samples. Proteins were removed from analysis if they did not meet the validation criteria (described in the methods) or, if they met the validation criteria but were not present in at least two biological samples. After removing proteins not meeting these criteria, the number of spectra for identical peptide ions was normalized as described in the methods. After normalization, 173 proteins remained in PPD-S2. Of these 173 proteins, 108 were common to PPD-RT23, and 120 were common to PPD-KIT for comparison. Analysis of global clustering between the expression level for identical genes demonstrated that biological replicates clustered together and that PPD-RT23 was more similar to PPD-KIT than either were to PPD-S2 (Fig. 3). Analysis of the paired datasets demonstrated 28 and 17 proteins were significantly different ($p<0.01$) between PPD-S2 and PPD-RT23 or PPD-S2 and PPD-KIT, and an additional 31 proteins for each pair that were significantly different with $p<0.05$ (Fig. 3). Specific analysis of relative quantities

Table 2. Dominant protein representatives identified in PPD-S2

PPD digestion	Protein name	No. of spectra (quantitative value)	Total weighted spectra (%)
Trypsin	Cochaperonin GroES	512	26.1
	Chaperonin GroEL	378	19.2
	Heat shock protein HSPX (ACR)	159	8.1
	Molecular chaperone DnaK	88	4.5
	Elongation factor TU	51	2.6
	Alanine- and proline-rich secreted protein APA (MPT-32)	48	2.4
	Secreted l-alanine dehydrogenase ALD	46	2.3
	Acyl carrier protein	40	2.0
	10 KDA culture filtrate antigen EsxB (CFP10)	34	1.7
	Thioredoxin TRXC (MPT46)	33	1.7
Chymotrypsin	Cochaperonin GroES	383	19.8
	Acyl carrier protein	126	6.5
	Hypothetical protein Rv0020c	116	6.0
	Chaperonin GroEL	105	5.4
	Molecular chaperone DnaK	89	4.6
	Catalase-peroxidase-peroxynitritase (KATG)	89	4.6
	Immunogenic protein MPT63	58	3.0
	Conserved hypothetical protein CFP17	58	3.0
	10 KDA culture filtrate antigen EsxB (CFP10)	53	2.7
	Thiol peroxidase	47	2.4

of the ten dominant protein representatives found in PPD-S2 (Table 2) versus PPD-RT23 or PPD-KIT, demonstrated that four protein representatives were present in different quantities in both PPD-RT23 and PPD-KIT versus PPD-S2 (Table 3), including two proteins, DnaK and ALD, present in lower quantities in both PPD-RT23 and PPD-KIT versus PPD-S2, and one protein, EsxB (CFP-10), present in higher quantities in both PPD-RT23 and PPD-KIT versus PPD-S2 (Table 3). Given the known potential of EsxB to induce potent, even cytotoxic DTH responses [60], the contribution of other Esx proteins to the immunopathogenesis (reviewed in Brodin et al. [61]) and our findings of severe inflammatory responses for PPD-RT23 and PPD-KIT (Fig. 2), the relative quantities of other members of the Esx family were examined. Five additional Esx proteins were present in the PPD preparations (EsxA, L, O, G, and K), and for all five, the relative quantity of each protein was significantly greater ($p<0.05$) in both PPD-RT23 and PPD-KIT versus PPD-S2 (Table 3).

4 Discussion

Despite significant advances in tuberculosis control since the first use of tuberculin as a diagnostic reagent, this disease remains a major global health issue. One of the most pressing issues is improved diagnostics. An alternative to PPD for diagnosis of tuberculosis is the use of interferon gamma release assays (IGRAs). These tests measure the cellular immune response through the release of interferon gamma after stimulation of peripheral blood mononuclear cells collected from suspected tuberculosis patients with *M. tuberculosis*-specific proteins/peptides. As a result, IGRAs are exceptionally specific and sensitive, however they require significant lab infrastructure and are cost prohibitive in resource limited countries. The PPD skin test is also highly sensitive and in contrast to the IGRAs are inexpensive, stable in a range of environmental conditions [62,63], and can be administered in the field. However, PPD is not widely applied for tuberculosis diagnosis in those regions with the greatest burden of disease because of its inability to differentiate between active and latent disease and continuing concerns with specificity.

A major impediment to developing a better skin test antigen has been a lack of knowledge as to the molecular composition of PPD and the contribution of individual gene products. Early studies on the definition and standardization of PPD led Affronti to hypothesize that specific qualities of PPD are essential for its immunological activity: (i) PPD must be prepared from denatured material to alleviate sensitization from repeated administration; (ii) PPD represents protein aggregates and not individually resolvable products; and (iii) the biological activity of PPD is not attributable to a single protein [50]. Our studies of human PPD derived from *M. tuberculosis* via the process described by Seibert [4] have in part tested these hypotheses and clearly demonstrated that PPD is a complex mixture of denatured proteins and protein fragments representing at least 6.0% of the proteins encoded on the *M. tuberculosis* genome. Moreover, even with modern 2D-LC approaches the complexity of PPD did not allow for clean resolution of individual peptides or for a specific peptide to be found in only one 2D-LC fraction. The denatured state and complexity of PPD also explains why previous investigators were unable to define more than a few major constituents. The complexity and form of the products in PPD likely resulted in the misidentification of PPD proteins, such as the 9.5 kDa prod-

Table 3. Comparison of dominant protein representatives and Esx proteins in PPDs

PPD comparison	Protein name	*p*-value	Fold change relative to PPD-S2[a)]
PPD-RT23 versus PPD-S2			
RAT-PPD-dominant proteins	Cochaperonin GroES	NS	ND
	Chaperonin GroEL	<0.01	2.9
	Heat shock protein HSPX (ACR)	NS	ND
	Molecular chaperone DnaK	<0.01	4.9
	Elongation factor TU	<0.01	7.4
	Alanine- and proline-rich secreted protein APA (MPT-32)	<0.01	−3.6
	Secreted L-alanine dehydrogenase ALD	<0.05	Detected in PPD-S2 only
	Acyl carrier protein	NS	ND
	10 KDA culture filtrate antigen EsxB (CFP10)	<0.01	−2.9
	Thioredoxin TRXC (MPT46)	<0.05	2.1
Esx proteins	EsxA	<0.05	−2.1
	EsxL	<0.01	−3.9
	EsxO	<0.01	−10.1
	EsxG	<0.01	Not detected in PPD−S2
	EsxK	<0.01	Not detected in PPD-S2
PPD-KIT versus PPD-S2			
RAT-PPD-dominant proteins	Cochaperonin GroES	NS	ND
	Chaperonin GroEL	NS	ND
	Heat shock protein HSPX (ACR)	<0.01	2.3
	Molecular chaperone DnaK	<0.05	4.9
	Elongation factor TU	<0.05	−1.7
	Alanine- and proline-rich secreted protein APA (MPT-32)	NS	ND
	Secreted L-alanine dehydrogenase ALD	<0.05	Detected in PPD-S2 only
	Acyl carrier protein	<0.05	1.0
	10 KDA culture filtrate antigen EsxB (CFP10)	<0.01	−8.2
	Thioredoxin TRXC (MPT46)	NS	ND
Esx proteins	EsxA	<0.05	−5.1
	EsxL	<0.05	−7.3
	EsxO	<0.01	−9.4
	EsxG	<0.01	Not detected in PPD-S2
	EsxK	<0.05	Not detected in PPD-S2

NS, not significant; ND, not determined.
a) Fold change relative to PPD-S2, where a positive fold change indicates significantly more counted spectra in PPD-S2 and a negative fold change indicates significantly more counted spectra in either PPD-RT23 or PPD-KIT.

uct of PPD erroneously identified by Kuwabara [11], that is now known not to be a true gene product of *M. tuberculosis* [35, 36]. Another early effort to characterize the composition of PPD was based on antibodies to *M. tuberculosis* proteins. Specifically, Rv0350 (DnaK) and Rv0440 (GroEL2) were described as components of PPD using polyclonal sera with immunoelectrophoresis [64]. Previous 2D-PAGE analysis of PPD prepared by SSI revealed an unresolved mixture of denatured proteins, similar to what we observed [9]. However, this earlier study was able to differentiate two low molecular mass proteins that were identified as Rv3418c (GroES) and Rv0652 (L7/L2 50 s ribosomal protein). Based on our analyses, all of these proteins were present in the PPD-S2 and three (DnaK, GroEL, and GroES) were identified as dominant products. Coler et al. purified from PPD a low molecular weight protein termed DPPD that induced a significant DTH response in tuberculosis patients [8]. It should be noted, however, that a standard PPD was not used to isolate DPPD, and unlike PPD-S2 or other PPD standards the PPD used by Coler and colleagues produced a distinct banding pattern by SDS-PAGE. Most recently, proteomic methodologies similar to those applied here were used to analyze the composition of PPD derived from *M. bovis*, a close relative of *M. tuberculosis* [65]. Two separate *M. bovis* PPD preparations were evaluated and a total of 116 proteins representatives were identified. The difference in the total number of protein representatives identified in PPD-S2 (240) and that for the *M. bovis* PPD preparations (116) is likely a reflection of the methodologies used. We utilized 2D-LC separation of trypsin and chymotrypsin digested PPD-S2, while the evaluation of *M. bovis* PPD was performed with peptides derived from trypsin digests of gel slices after SDS-PAGE separation of PPD. Thus, the large amount of starting materials used in the evaluation of PPD-S2, the inclusion of both trypsin and chymotrypsin digests, and the extensive fractionation we employed likely resulted in the identification of more protein representatives. Of the 116 protein representatives in the *M. bovis* PPD preparations, 80 (69%) were also identified in our analyses of the

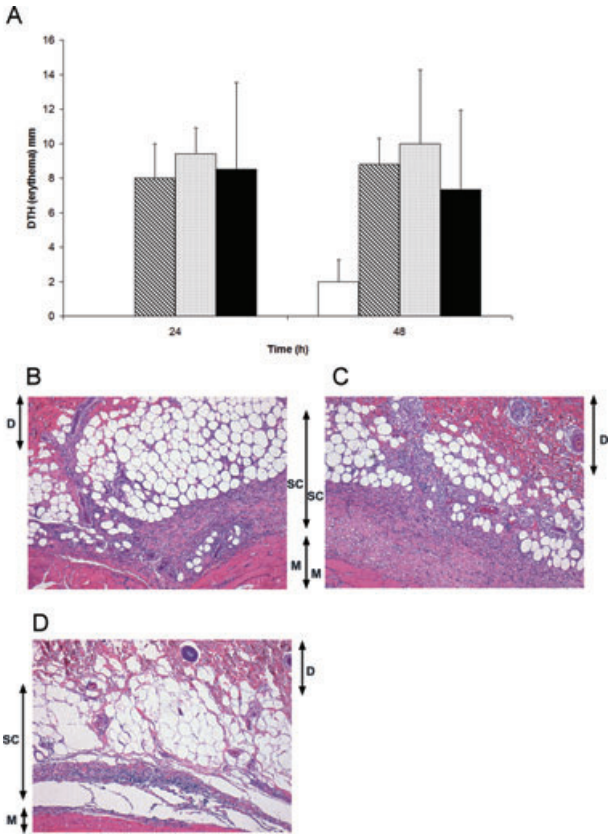

Figure 2. Analysis of the DTH response to three preparations of PPD. (A) Strength of the DTH response as measured by erythematous reactions at PPD injection sites of guinea pigs infected with *M. tuberculosis* for 10 wk. Measurements were made at 24 and 48 h postintradermal injection of PPD-S2 (diagonally slashed bar), PPD-KIT (speckled bar), and PPD-RT23 (black bar). The saline control is represented with the open bar. All data are average values and standard deviation of five guinea pigs per PPD preparation. (B–D) are photomicrographs of histological preparations of dermal tissue from PPD-S2 (B), PPD-KIT (C), and PPD-RT23 (D) injection sites. Microscopic analysis of tissue demonstrated extensive inflammation typical of a DTH response for all PPD preparations. For reference, layers of the integumentary system are identified; dermis (D), subcutis (SC), and muscle (M). All photomicrographs are at 40× magnification.

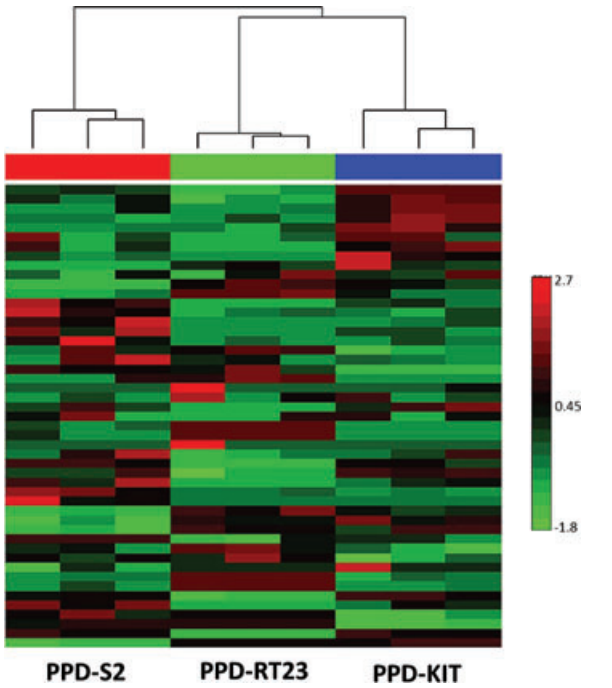

Figure 3. HCA heat map of the protein representatives present in the PPD samples. Each row represents individual proteins and each column represents a PPD sample, each of which (PPD-S2, PPD-RT23, and PPD-KIT) were run in triplicate. Cells are colored by z-score that represent the deviation for each protein in each sample from the mean spectral count for that protein. The complete list of proteins compared is available (Supporting Information Table S3).

M. tuberculosis PPD. Likewise, seven of the ten most abundant protein representatives identified in RAT- or RAC-PPD preparations based on spectral counting [41] were also identified as highly abundant in the *M. bovis* PPD using the empAI (exponentially modified protein abundance index) function of MASCOT [66]. More interestingly, the seven highly abundant protein representatives that correlated to those in *M. bovis* PPD were the same seven found to be highly abundant in both the RAT- and RAC-PPD preparations (Table 2). Thus, although there are considerable differences in the experimental approaches and likely the methods used to generate the various PPD preparations it would appear that the most dominant products of PPD remain consistent.

It is widely accepted that variability exists in the potency of different PPD preparations [58]. However, no studies have been published to define compositional differences among PPD standards or commercially manufactured PPDs used in human diagnostics. Given the complexity of PPD and the state of the PPD proteins, a protein-by-protein comparison of the composition of individual PPD preparations would be difficult based on current proteomic methods. The proteomic evaluation of *M. bovis* PPD included the comparison of PPDs manufactured in Brazil and the United Kingdom, and showed that only 33 of the 116 total protein representatives were present in both preparations [65]. Additionally, only four of the ten most abundant protein representatives in the two preparations overlapped. The protocols used to generate the Brazilian and United Kingdom PPDs differed significantly and this likely contributed to the modest overlap (28%) in identifiable products. However, it was not possible to determine how experimental variability in the proteomic analysis of each sample contributed to the lack of concordance between the two *M. bovis* PPD preparations. In contrast to the protein-by-protein comparison our evaluation of PPD-S2, PPD-RT23, and PPD-KIT utilized nanospray-LTQ tandem MS with spectral counting and comparative evaluation of proteins after quantile normalization of individual peptides. By

this method, 72% (173) of the proteins identified from 2D-LC analysis of PPD-S2 could be compared between replicate samples of PPD-S2, and 45% (108) and 50% (120) of these proteins could be compared between PPD-RT23 and PPD-KIT versus PPD-S2, respectively. This analysis demonstrated that the other two PPD preparations differed considerably from PPD-S2. These relative compositional differences also correlated to differences in the histopathology of the DTH response to the PPD preparations, but not in the measurement of erythema. Discreet analysis of the differences in protein composition identified relative increases in the Esx proteins present in PPD-RT23 and PPD-KIT. Although speculative, the increased abundance of this protein family in PPD-RT23 and PPD-KIT may contribute to the increased inflammatory responses observed when these two reagents were administered in this guinea pig model. Thus, these series of experiments have demonstrated methods by which individual preparations of PPD can be compared both at a molecular and biological level, and could be applied to the further standardization of PPD. With this base knowledge and approach, it is also possible to extend the analyses of PPD preparations such that individual protein representatives with quantifiable differences between PPD preparations are identified and the impact that specific compositional differences have on the biological activity of PPD can be measured at a cellular level.

Elucidating the relative quantities of individual protein representative in PPD-S2 led to the recognition of a disproportionate abundance of the HSPs (Acr, DnaK, GroEL, and GroES), and given this preponderance it is likely the HSPs significantly influence the biological activity of PPD. A lack of specificity has been cited as one of the major limitations to the use of PPD as a diagnostic for tuberculosis in endemic settings [67] and the potential of cross-reactive epitopes on the highly conserved HSPs [68] would be expected to account for the reported cross-reactivity to PPD. However, a recent retrospective review of studies conducted since 1966 argues that PPD does possess high specificity, even in individuals vaccinated with *M. bovis* BCG (bacillus Calmette-Guérin) as infants and skin tested at greater than 10 years of age [69]. This review also revealed that exposure to nontuberculosis mycobacteria (NTM) does not significantly contribute to false positive PPD responses unless the individual is in a region with a high prevalence of NTM and low prevalence of *M. tuberculosis* infections. Thus, the data on the composition of PPD when coupled with this retrospective evaluation of clinical studies would suggest that the abundance HSPs in PPD is not a shortcoming of this diagnostic reagent. On the other hand, recent evaluation of bacterial HSPs and their interaction with the innate and adaptive immune response [70–72] would argue that these products may actually enhance sensitivity of PPD to a level that cannot be achieved with individual purified *M. tuberculosis* proteins predicted to provide greater specificity. Moreover, the abundance of the HSPs and their chaperone activity [73] would explain the exquisite solubility of PPD; a property that would not be expected given the protein aggregation as observed by SDS-PAGE and the denaturing conditions used to generate PPD. Given the new understanding of the protein representatives that comprise PPD, these hypotheses are now being tested. Specifically, the PPD compositional data are being used to develop second-generation skin test antigens that retain the qualities of PPD but are well defined in composition [74].

The authors wish to thank Preston Hill for assistance with mass spectrometry. This work was supported by the NIH, NIAID Contract N01-AI-75320 (JTB), NIH, NIAID contract N01-AI-40091c (KMD), and a Monfort Professorship (JTB). YSC was supported by the Postdoctoral Fellowship Program of Korea Research Foundation Grant (MOEHRD, Basic Research Promotion Fund) KRF-2004-214-E00034. PRoteomics IDEntifications database (PRIDE) data conversions and storage made available at http://www.ebi.ac.uk/pride/; PMID accession # 19587657.

The authors have declared no conflict of interest.

5 References

[1] Koch, R., Weitere Mittheilungen uber das Tuberkulin. *Dt. Med. Wochenschr.* 1891, *17*, 1189–1192.

[2] von Pirquet, C., Freguency of tuberculosis in childhood. *J. Am. Med. Assoc.* 1909, *52*, 675–678.

[3] Seibert, F. B., The isolation of a crystalline protein with tuberculin activity. *Science* 1926, *63*, 619–620.

[4] Seibert, F. B., Glenn, J. T., Tuberculin purified protein derivative. Preparation and analysis of a large quantity for standard. *Am. Rev. Tubercul.* 1941, *44*, 9–25.

[5] Comstock, G. W., Edwards, L. B., Philip, R. N., Winn, W. A., A comparison in the United States of America of two tuberculins, PPD-S and RT23. *Bull. World Health Organ.* 1964, *31*, 161–170.

[6] Guld, J., Bentzon, M. W., Bleiker, M. A., Griep, W. A. et al., Standardization of a new batch of purified tuberculin (PPD) intended for international use. *Bull. World Health Organ.* 1958, *19*, 845–951.

[7] Villarino, M. E., Brennan, M. J., Nolan, C. M., Catanzaro, A. et al., Comparison testing of current (PPD-SI) and proposed (PPD-S2) reference tuberculin standards. *Am. J. Respir. Crit. Care Med.* 2000, *161*, 1167–1171.

[8] Coler, R. N., Skeiky, Y. A., Ovendale, P. J., Vedvick, T. S. et al., Cloning of a *Mycobacterium tuberculosis* gene encoding a purifed protein derivative protein that elicits strong tuberculosis-specific delayed-type hypersensitivity. *J. Infect. Dis.* 2000, *182*, 224–233.

[9] Kitaura, H., Kinomoto, M., Yamada, T., Ribosomal protein L7 included in tuberculin purified protein derivative (PPD) is a major heat-resistant protein inducing strong delayed-type hypersensitivity. *Scand. J. Immunol.* 1999, *50*, 580–587.

[10] Kuwabara, S., Purification and properties of tuberculin-active protein from *Mycobacterium tuberculosis*. *J. Biol. Chem.* 1975, *250*, 2556–2562.

[11] Kuwabara, S., Amino-acid sequence of tuberculin-active protein from *Mycobacterium tuberculosis*. *J. Biol. Chem.* 1975, *250*, 2563–2568.

[12] Malen, H., Berven, F. S., Fladmark, K. E., Wiker, H. G., Comprehensive analysis of exported proteins from *Mycobacterium tuberculosis* H37Rv. *Proteomics* 2007, *7*, 1702–1718.

[13] Mawuenyega, K. G., Forst, C. V., Dobos, K. M., Belisle, J. T. et al., Mycobacterium tuberculosis functional network analysis by global subcellular protein profiling. *Mol. Biol. Cell* 2005, *16*, 396–404.

[14] Rosenkrands, I., Weldingh, K., Jacobsen, S., Hansen, C. V. et al., Mapping and identification of *Mycobacterium tuberculosis* proteins by two-dimensional gel electrophoresis, microsequencing and immunodetection. *Electrophoresis* 2000, *21*, 935–948.

[15] Urquhart, B. L., Cordwell, S. J., Humphery-Smith, I., Comparison of predicted and observed properties of proteins encoded in the genome of *Mycobacterium tuberculosis* H37Rv. *Biochem. Biophys. Res. Commun.* 1998, *253*, 70–79.

[16] Betts, J. C., Dodson, P., Quan, S., Lewis, A. P. et al., Comparison of the proteome of *Mycobacterium tuberculosis* strain H37Rv with clinical isolate CDC 1551. *Microbiology* 2000, *146*(Pt 12), 3205–3216.

[17] He, X. Y., Zhuang, Y. H., Zhang, X. G., Li, G. L., Comparative proteome analysis of culture supernatant proteins of *Mycobacterium tuberculosis* H37Rv and H37Ra. *Microbes Infect.* 2003, *5*, 851–856.

[18] Jiang, X., Zhang, Y., Zhang, W., Gao, F. et al., Identification of unique genetic markers in Rv0927c among *Mycobacterium tuberculosis* W-Beijing strains. *Microbes Infect.* 2007, *9*, 241–246.

[19] Jungblut, P. R., Schaible, U. E., Mollenkopf, H. J., Zimny-Arndt, U. et al., Comparative proteome analysis of *Mycobacterium tuberculosis* and *Mycobacterium bovis* BCG strains: towards functional genomics of microbial pathogens. *Mol. Microbiol.* 1999, *33*, 1103–1117.

[20] Mattow, J., Jungblut, P. R., Schaible, U. E., Mollenkopf, H. J. et al., Identification of proteins from *Mycobacterium tuberculosis* missing in attenuated *Mycobacterium bovis* BCG strains. *Electrophoresis* 2001, *22*, 2936–2946.

[21] Pheiffer, C., Betts, J. C., Flynn, H. R., Lukey, P. T. et al., Protein expression by a Beijing strain differs from that of another clinical isolate and *Mycobacterium tuberculo*sis H37Rv. *Microbiology* 2005, *151*, 1139–1150.

[22] Betts, J. C., Lukey, P. T., Robb, L. C., McAdam, R. A. et al., Evaluation of a nutrient starvation model of *Mycobacterium tuberculosis* persistence by gene and protein expression profiling. *Mol. Microbiol.* 2002, *43*, 717–731.

[23] Boon, C., Li, R., Qi, R., Dick, T., Proteins of *Mycobacterium bovis* BCG induced in the Wayne dormancy model. *J. Bacteriol.* 2001, *183*, 2672–2676.

[24] Cho, S. H., Goodlett, D., Franzblau, S., ICAT-based comparative proteomic analysis of non-replicating persistent *Mycobacterium tuberculosis*. *Tuberculosis (Edinb.)* 2006, *86*, 445–460.

[25] Florczyk, M. A., McCue, L. A., Stack, R. F., Hauer, C. R. et al., Identification and characterization of mycobacterial proteins differentially expressed under standing and shaking culture conditions, including Rv2623 from a novel class of putative ATP-binding proteins. *Infect. Immun.* 2001, *69*, 5777–5785.

[26] Rosenkrands, I., Slayden, R. A., Crawford, J., Aagaard, C. et al., Hypoxic response of *Mycobacterium tuberculosis* studied by metabolic labeling and proteome analysis of cellular and extracellular proteins. *J. Bacteriol.* 2002, *184*, 3485–3491.

[27] Starck, J., Kallenius, G., Marklund, B. I., Andersson, D. I. et al., Comparative proteome analysis of *Mycobacterium tuberculosis* grown under aerobic and anaerobic conditions. *Microbiology* 2004, *150*, 3821–3829.

[28] Wong, D. K., Lee, B. Y., Horwitz, M. A., Gibson, B. W., Identification of fur, aconitase, and other proteins expressed by *Mycobacterium tuberculosis* under conditions of low and high concentrations of iron by combined two-dimensional gel electrophoresis and mass spectrometry. *Infect. Immun.* 1999, *67*, 327–336.

[29] Yuan, Y., Crane, D. D., Barry, C. E., 3rd, Stationary phase-associated protein expression in *Mycobacterium tuberculosis*: function of the mycobacterial alpha-crystallin homolog. *J. Bacteriol.* 1996, *178*, 4484–4492.

[30] Covert, B. A., Spencer, J. S., Orme, I. M., Belisle, J. T., The application of proteomics in defining the T cell antigens of *Mycobacterium tuberculosis*. *Proteomics* 2001, *1*, 574–586.

[31] Malen, H., Berven, F. S., Softeland, T., Arntzen, M. O. et al., Membrane and membrane-associated proteins in Triton X-114 extracts of *Mycobacterium bovis* BCG identified using a combination of gel-based and gel-free fractionation strategies. *Proteomics* 2008, *8*, 1859–1870.

[32] Sable, S. B., Kumar, R., Kalra, M., Verma, I. et al., Peripheral blood and pleural fluid mononuclear cell responses to low-molecular-mass secretory polypeptides of *Mycobacterium tuberculosis* in human models of immunity to tuberculosis. *Infect. Immun.* 2005, *73*, 3547–3558.

[33] Samanich, K. M., Belisle, J. T., Sonnenberg, M. G., Keen, M. A. et al., Delineation of human antibody responses to culture filtrate antigens of *Mycobacterium tuberculosis*. *J. Infect. Dis.* 1998, *178*, 1534–1538.

[34] Sartain, M. J., Slayden, R. A., Singh, K. K., Laal, S. et al., Disease state differentiation and identification of tuberculosis biomarkers via native antigen array profiling. *Mol. Cell. Proteomics* 2006, *5*, 2102–2113.

[35] Wiker, H. G., Unmatched sequences in public databases—exemplified by tuberculin-active protein. *Scand. J. Immunol.* 2004, *59*, 607–608.

[36] Cole, S. T., Brosch, R., Parkhill, J., Garnier, T. et al., Deciphering the biology of *Mycobacterium tuberculosis* from the complete genome sequence. *Nature* 1998, *393*, 537–544.

[37] Washburn, M. P., Wolters, D., Yates, J. R., 3rd, Large-scale analysis of the yeast proteome by multidimensional protein identification technology. *Nat. Biotechnol.* 2001, *19*, 242–247.

[38] Fenn, J. B., Mann, M., Meng, C. K., Wong, S. F. et al., Electrospray ionization for mass spectrometry of large biomolecules. *Science* 1989, *246*, 64–71.

[39] Hirosawa, M., Hoshida, M., Ishikawa, M., Toya, T., MASCOT: multiple alignment system for protein sequences based

on three-way dynamic programming. *Comput. Appl. Biosci.* 1993, *9*, 161–167.

[40] Link, A. J., Eng, J., Schieltz, D. M., Carmack, E. et al., Direct analysis of protein complexes using mass spectrometry. *Nat. Biotechnol.* 1999, *17*, 676–682.

[41] Paoletti, A. C., Parmely, T. J., Tomomori-Sato, C., Sato, S. et al., Quantitative proteomic analysis of distinct mammalian Mediator complexes using normalized spectral abundance factors. *Proc. Natl. Acad. Sci. USA* 2006, *103*, 18928–18933.

[42] Gygi, S. P., Rist, B., Gerber, S. A., Turecek, F. et al., Quantitative analysis of complex protein mixtures using isotope-coded affinity tags. *Nat. Biotechnol.* 1999, *17*, 994–999.

[43] Aitken, A., Learnmonth, M., in: Walker, J. M. (Ed.), *The Protein Protocols Handbook*, Humana Press, Totowa, NJ 2002, pp. 455–456.

[44] Lee, B. Y., Hefta, S. A., Brennan, P. J., Characterization of the major membrane protein of virulent *Mycobacterium tuberculosis*. *Infect. Immun.* 1992, *60*, 2066–2074.

[45] Hellman, U., Wernstedt, C., Gonez, J., Heldin, C. H., Improvement of an in-gel digestion procedure for the micropreparation of internal protein-fragments for amino-acid sequencing. *Anal. Biochem.* 1995, *224*, 451–455.

[46] Vizcaino, J. A., Cote, R., Reisinger, F., Barsnes, H. et al., The Proteomics Identifications database: 2010 update. *Nucleic Acids Res.* 2010, *38*, D736–D742.

[47] Paoletti, A. C., Parmely, T. J., Tomomori-Sato, C., Sato, S. et al., Quantitative proteomic analysis of distinct mammalian Mediator complexes using normalized spectral abundance factors. *Proc. Natl. Acad. Sci. USA* 2006, *103*, 18928–18933.

[48] Searle, B. C., Scaffold: a bioinformatic tool for validating MS/MS-based proteomic studies. *Proteomics* 2010, *10*, 1265–1269.

[49] Mehaffy, C., Hess, A., Prenni, J. E., Mathema, B. et al., Descriptive proteomic analysis shows protein variability between closely related clinical isolates of *Mycobacterium tuberculosis*. *Proteomics* 2010, *10*, 1966–1984.

[50] Affronti, L. F., in: Bendinelli, M., Friedman, H. (Eds.), *Mycobacterium Tuberculosis Interactions with the Immune Sysytem*, Plenum Press, New York 1988, pp. 1–37.

[51] Aebersold, R., Goodlett, D. R., Mass spectrometry in proteomics. *Chem. Rev.* 2001, *101*, 269–295.

[52] Nesvizhskii, A. I., Keller, A., Kolker, E., Aebersold, R., A statistical model for identifying proteins by tandem mass spectrometry. *Anal. Chem.* 2003, *75*, 4646–4658.

[53] Belisle, J. T., Braunstein, M., Rosenkrands, I., Andersen, P. (Eds.), *The Proteome of Mycobacterium Tuberculosis*, American Society for Microbiology, Washington, DC 2005.

[54] Dobos, K. M., Belisle, J. T. (Eds.), *Proteomics of Mycobacterium Tuberculosis*, Wiley-VCH, Darmstadt 2008.

[55] Vita, R., Zarebski, L., Greenbaum, J. A., Emami, H., Hoof, I. et al., The immune epitope database 2.0. *Nucleic Acids Res.* 2010, *38*, D854–D862.

[56] Sable, S. B., Plikaytis, B. B., Shinnick, T. M., Tuberculosis subunit vaccine development: impact of physicochemical properties of mycobacterial test antigens. *Vaccine* 2007, *25*, 1553–1566.

[57] Cho, S., Mehra, V., Thoma-Uszynski, S., Stenger, S. et al., Antimicrobial activity of MHC class I-restricted CD8+ T cells in human tuberculosis. *Proc. Natl. Acad. Sci. USA* 2000, *97*, 12210–12215.

[58] Lee, E., Holzman, R. S., Evolution and current use of the tuberculin test. *Clin. Infect. Dis.* 2002, *34*, 365–370.

[59] Basaraba, R. J., Izzo, A. A., Brandt, L., Orme, I. M., Decreased survival of guinea pigs infected with *Mycobacterium tuberculosis* after multiple BCG vaccinations. *Vaccine* 2006, *24*, 280–286.

[60] Reece, S. T., Stride, N., Ovendale, P., Reed, S. G. et al., Skin test performed with highly purified *Mycobacterium tuberculosis* recombinant protein triggers tuberculin shock in infected guinea pigs. *Infect. Immun.* 2005, *73*, 3301–3306.

[61] Brodin, P., Rosenkrands, I., Andersen, P., Cole, S. T. et al., ESAT-6 proteins: protective antigens and virulence factors? *Trends Microbiol.* 2004, *12*, 500–508.

[62] Haslov, K., Tuberculin PPD RT23 is stable: quality control data cannot be denied. *Int. J. Tuberc. Lung Dis.* 1998, *2*, 946.

[63] Haslov, K., Ponce-de-Leon Rosales, S., Rangel-Frausto, S., Olesen Larsen, S., Tuberculin PPD RT23: still going strong. *Int. J. Tuberc. Lung Dis.* 1998, *2*, 793–795.

[64] Harboe, M., Antigens of PPD, old tuberculin, and autoclaved *Mycobacterium bovis* BCG studied by crossed immunoelectrophoresis. *Am. Rev. Respir. Dis.* 1981, *124*, 80–87.

[65] Borsuk, S., Newcombe, J., Mendum, T. A., Dellagostin, O. A. et al., Identification of proteins from tuberculin purified protein derivative (PPD) by LC-MS/MS. *Tuberculosis (Edinb.)* 2009, *89*, 423–430.

[66] Ishihama, Y., Oda, Y., Tabata, T., Sato, T. et al., Exponentially modified protein abundance index (emPAI) for estimation of absolute protein amount in proteomics by the number of sequenced peptides per protein. *Mol. Cell Proteomics* 2005, *4*, 1265–1272.

[67] Perkins, M. D., New diagnostic tools for tuberculosis. *Int. J. Tuberc. Lung Dis.* 2000, *4*, S182–S188.

[68] Hussain, R., Shahid, F., Zafar, S., Dojki, M. et al., Immune profiling of leprosy and tuberculosis patients to 15-mer peptides of *Mycobacterium leprae* and M. tuberculosis GroES in a BCG vaccinated area: implications for development of vaccine and diagnostic reagents. *Immunology* 2004, *111*, 462–471.

[69] Farhat, M., Greenaway, C., Pai, M., Menzies, D., False-positive tuberculin skin tests: what is the absolute effect of BCG and non-tuberculous mycobacteria? *Int. J. Tuberc. Lung Dis.* 2006, *10*, 1192–1204.

[70] Floto, R. A., MacAry, P. A., Boname, J. M., Mien, T. S. et al., Dendritic cell stimulation by mycobacterial Hsp70 is mediated through CCR5. *Science* 2006, *314*, 454–458.

[71] Javid, B., MacAry, P. A., Lehner, P. J., Structure and function: heat shock proteins and adaptive immunity. *J. Immunol.* 2007, *179*, 2035–2040.

[72] Tobian, A. A., Canaday, D. H., Harding, C. V., Bacterial heat shock proteins enhance class II MHC antigen processing and

presentation of chaperoned peptides to CD4+ T cells. *J. Immunol.* 2004, *173*, 5130–5137.

[73] Qamra, R., Mande, S. C., Coates, A. R. M., Henderson, B., The unusual chaperonins of *Mycobacterium tuberculosis*. *Tuberculosis* 2005, *85*, 385–394.

[74] Yang, H., Troudt, J., Grover, A., Arnett, K. et al., Three protein cocktails mediate delayed-type hypersensitivity responses indistinguishable from that elicited by purified protein derivative in the guinea pig model of *Mycobacterium tuberculosis* infection. *Infect. Immun.* 2011, *79*, 716–723.

